AIAA 99-3998
Modified Dynamic Inversion to Control Large Flexible Aircraft – What's Going On?

Irene M. Gregory
NASA Langley Research Center
Hampton, VA

AIAA Guidance, Navigation, and Control Conference
August 9-11,1999 /Portland, OR

For permission to copy or republish, contact the American Institute of Aeronautics and Astronautics
1801 Alexander Bell Drive, Suite 500, Reston, VA, 20191-4344

MODIFIED DYNAMIC INVERSION TO CONTROL LARGE FLEXIBLE AIRCRAFT – WHAT'S GOING ON?

Irene M. Gregory
Research Engineer, Flight Dynamics and Control Division
NASA Langley Research Center
Hampton, VA

Abstract

High performance aircraft of the future will be designed lighter, more maneuverable, and operate over an ever expanding flight envelope. One of the largest differences from the flight control perspective between current and future advanced aircraft is elasticity. Over the last decade, dynamic inversion methodology has gained considerable popularity in application to highly maneuverable fighter aircraft, which were treated as rigid vehicles. This paper explores dynamic inversion application to an advanced highly flexible aircraft.

An initial application has been made to a large flexible supersonic aircraft. In the course of controller design for this advanced vehicle, modifications were made to the standard dynamic inversion methodology. The results of this application were deemed rather promising. An analytical study has been undertaken to better understand the nature of the made modifications and to determine its general applicability. This paper presents the results of this initial analytical look at the modifications to dynamic inversion to control large flexible aircraft.

Introduction

The advanced aircraft under consideration is a next generation supersonic transport aircraft, which due to aerodynamic considerations will be long and slender and because of economics must be as light as possible. These factors contribute to making this aircraft very flexible with the first few elastic modes lying within the bandwidth of the traditional flight control system. Traditionally, any aircraft flexibility that had to be addressed directly has been always handled by designing a separate structural mode control system to augment the standard flight control [1]. This approach while not optimal, has performed adequately in the past but does not fulfill the requirements for the new generation of advanced aircraft [2]. The new generation of flexible aircraft requires a new integrated approach in order to effectively control elasticity while providing the best available performance.

In order to address this newly defined problem of integrated flight/structural mode control for an advanced aircraft, the method of dynamic inversion is considered. Over the last decade, dynamic inversion methodology has gained considerable popularity in application to highly maneuverable fighter aircraft [3, 4, 5] which makes it a candidate that might benefit the advanced highly flexible aircraft of the future. The attractiveness of this methodology lies in the fact that the inherent nonlinearities of the problem are explicitly considered. In other words, a nonlinear control law is designed that globally reduces the aircraft dynamics of interest into a set of integrators and thus, allows one linear controller to provide desired response throughout the flight envelope. This eliminates the need for extensive linearization of the aircraft model for different flight conditions, design of individual controllers for each of these conditions, and finally performing gain scheduling, which is typically an ad hoc and time consuming procedure, to link the individual controllers over the flight envelope. However, since no methodology is a panacea for control design, dynamic inversion has some associated issues, such as robustness, stability, and onboard aircraft model fidelity that must be carefully considered.

An initial application of dynamic inversion to a large flexible aircraft has been made with encouraging results [6]. These results, however, required certain modifications to be made to the standard dynamic inversion to handle flexibility. The paper discusses these modifications and shows analytically how they affect the dynamics. The original control design problem [6] dealt with a large, complicated model. In order to show useful results, the problem has been simplified for analytical work while still retaining essential characteristics. The simplification involved considering short period longitudinal dynamics with a single elastic mode and then going through the process of dynamic inversion both original and modified concept to show the affects on aircraft dynamics due to the introduced modifications. The complexity of the model was then gradually increased to include more dynamics.

*Copyright © 1999 by the American Institute of Aeronautics and Astronautics, Inc. No copyright is asserted in the United States under Title 17, U.S. Code. The U.S. Government has a royalty-free license to exercise all rights under the copyright claimed herein for Government Purposes. All other rights are reserved by the copyright owner.

The paper is organized as follows. The first section discusses the standard dynamic inversion results as applied to the short period plus an elastic mode linear equations of motion. The following section then deals with the modification introduced into the dynamic inversion that is the main result of this paper. The subsequent sections address the increasing complexity of the model by introducing full longitudinal dynamics and additional flexible modes respectively. The final section explores how uncertainty introduced into elastic mode frequency and damping, as was done in reference 6, influences closed loop dynamics that are found in the traditional rigid body frequency range. The conclusions that were drawn from this work then follow.

Throughout this paper the analysis considers the inner loop of the dynamic inversion only, i.e., the y to $\dot{y}^{des}$ portion. It is important to note that the nature of $\dot{y}^{des}$ impacts the overall closed loop dynamics but will not be discussed here. Also, the data plots shown here are normalized in order to be publishable.

Standard Dynamic Inversion

The aircraft model used to explore the analytical relationships considered in this section has the standard short period approximation plus an elastic mode [7] that is modified to show interaction between rigid and flexible body dynamics. The equations are given below

$$\begin{bmatrix} \dot{w} \\ \dot{q} \\ \ddot{\eta} \\ \dot{\eta} \end{bmatrix} = \begin{bmatrix} Z_w & Z_q & Z_{\dot{\eta}} & Z_\eta \\ M_w & M_q & M & M_\eta \\ E_w & E_q & -2\zeta\omega & -\omega^2 \\ 0 & 0 & 1 & 0 \end{bmatrix} \begin{bmatrix} w \\ q \\ \dot{\eta} \\ \eta \end{bmatrix} + \begin{bmatrix} Z_\delta & Z_{rcv} \\ M_\delta & M_{rcv} \\ E_\delta & E_{rcv} \\ 0 & 0 \end{bmatrix} \begin{bmatrix} \delta \\ RCV \end{bmatrix} \tag{1}$$

where η and $\dot{\eta}$ represent the generalized coordinate and its derivative, both of which are typically used to represent the flexible modal dynamics. The variables that are controlled, also subsequently referred to as control variable or CV, are pitch rate at the mean and the flexible motion at the pilot station, which is given by a difference between pitch rate at the pilot station (ps) and at a longitudinal mean axis (ma). Since the mean axis refers to an imaginary line that approximates the middle of a rigid vehicle and does not physically exist, it is approximated by a sensor measurement that shows the least flexible mode contamination. The pitch rate measurement provided by such sensor location is referred henceforth as q_{ma}. The equation describing the control variables is given by

$$y = \begin{bmatrix} q_{ma} \\ q_{ps} - q_{ma} \end{bmatrix} = \begin{bmatrix} 0 & 1 & \phi'_{ma} & 0 \\ 0 & 0 & \phi'_{ps} - \phi'_{ma} & 0 \end{bmatrix} \begin{bmatrix} w \\ q \\ \dot{\eta} \\ \eta \end{bmatrix} = \begin{bmatrix} 0 & 1 & \phi'_{ma} & 0 \\ 0 & 0 & \Delta\phi' & 0 \end{bmatrix} \begin{bmatrix} w \\ q \\ \dot{\eta} \\ \eta \end{bmatrix} \tag{2}$$

where ϕ' is the slope of the mode shape.

Applying the standard dynamic inversion to a set of linear equations in general gives us the following results.

$$\begin{aligned} \dot{x} &= Ax + Bu = Ax + B\left\{(CB)^{-1}\left(\dot{y}^{des} - CAx\right)\right\} \\ &= \left(A - B(CB)^{-1}CA\right)x + B(CB)^{-1}\dot{y}^{des} \\ &\rightarrow C\dot{x} = \dot{y} = \dot{y}^{des} \end{aligned} \tag{3}$$

Thus, applying equation 3 to the dynamics described by equations 1 and 2 gives the transfer function matrix for the closed loop

$$\frac{y}{\dot{y}^{des}} = \begin{bmatrix} 1/s & 0 \\ 0 & 1/s \end{bmatrix}. \tag{4}$$

The closed loop system dynamics from $\dot{y}^{des}$ to $\dot{y}$ are given by equation 5.

$$\begin{bmatrix} \dot{w} \\ \dot{q} \\ \ddot{\eta} \\ \dot{\eta} \end{bmatrix} = \begin{bmatrix} \overline{Z}_w & \overline{Z}_q & \overline{Z}_{\dot{\eta}} & \overline{Z}_\eta \\ 0 & 0 & 0 & 0 \\ 0 & 0 & 0 & 0 \\ 0 & 0 & 1 & 0 \end{bmatrix} \begin{bmatrix} w \\ q \\ \dot{\eta} \\ \eta \end{bmatrix} + \begin{bmatrix} \overline{Z}_{\dot{y}1} & \overline{Z}_{\dot{y}2} \\ 1 & \overline{M}_{\dot{y}2} \\ 0 & \overline{E}_{\dot{y}2} \\ 0 & 0 \end{bmatrix} \begin{bmatrix} \dot{y}_1 \\ \dot{y}_2 \end{bmatrix}^{des} \tag{5}$$

$$\begin{bmatrix} \dot{y}_1 \\ \dot{y}_2 \end{bmatrix} = \begin{bmatrix} \dot{y}_1^{des} + \left(\overline{M}_{\dot{y}2} + \phi'\overline{E}_{\dot{y}2}\right)\dot{y}_2^{des} \\ \Delta\phi'\overline{E}_{\dot{y}2}\dot{y}_2^{des} \end{bmatrix} = \begin{bmatrix} \dot{y}_1^{des} \\ \dot{y}_2^{des} \end{bmatrix}$$

where $\overline{M}_{\dot{y}2} = -\phi'\overline{E}_{\dot{y}2}$ and $\Delta\phi'\overline{E}_{\dot{y}2} = 1$

The set of closed loop poles, shown in expression 6 contains two poles at s=0 that correspond to the integrators shown in equation 4 plus those coinciding with the transmission zeros of the open loop system.

$$\left\{ \begin{aligned} & Z_w + Z_\delta\left(\frac{E_w M_{rcv} - E_{rcv} M_w}{E_{rcv} M_\delta - E_\delta M_{rcv}}\right) \\ & \quad + Z_{rcv}\left(\frac{E_\delta M_w - E_w M_\delta}{E_{rcv} M_\delta - E_\delta M_{rcv}}\right), \ 0, \ 0, \ 0 \end{aligned} \right\} \tag{6}$$

These are the internal or zero dynamics; one corresponding to the vertical velocity w, which is not directly controlled in the problem formulation, and the other to s=0. So the results are standard as expected when exact dynamic inversion is applied to an aircraft.

However, this methodology works well if the only interested is in controlling the dynamics from some commanded pitch rate coming from either pilot stick or an autopilot command, but it has no effect on controlling disturbances or improving robustness to model uncertainties that always exist.

Modified Dynamic Inversion

The presence of flexible modes in the close proximity to rigid body dynamics that are typically controlled raises a new set of challenges for the control engineer in utilizing dynamic inversion. In order to design a successful controller, the method of dynamic inversion must be modified to influence the damping of elastic modes so that the response to system disturbances and model uncertainties is acceptable. The analytical description of a simplified version of such a modification [6] is the main result of this paper.

The modification to dynamic inversion is introduced in the forward section of the dynamic inversion feedback loop and is illustrated in figure 1. Since the problem formulation is MIMO, a matrix W is introduced to limit the frequency range of the dynamics that are passed to the inverse of the effective control effectiveness matrix that produces actuator commands. In reference 6, the matrix W is diagonal consisting of second-order filters.

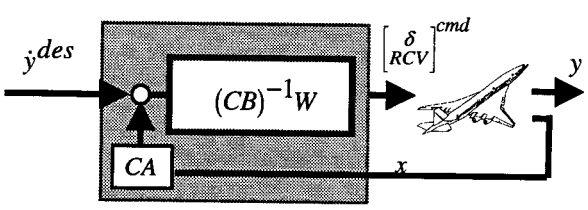

Figure 1. Modified dynamic inversion

In order to illustrate just how the described modification influences the closed loop dynamics several variations of the simplified open loop system and W are presented.

We first start by looking at SISO system dynamics and begin with short period dynamics only. Let W equal a first order filter. The closed loop dynamics and transfer function are then given in equation 7. Note that the right side of equation 7 is no longer a pure integrator as is the case in equation 4. The filter W in the loop introduces another pole-zero pair that precludes pole-zero cancellation resulting from the standard dynamic inversion. The movement of the poles with the changing value of a is illustrated in figure 2. For a>1, the non-integrator closed loop dynamics are concentrated around open loop poles, as follows from equation 7. On the other hand, for a<1, the short period dynamics become faster as both non-integrator poles move further into the left-half plane. It is interesting to note that as $1/a \to \infty$ the pole-zero cancellation is recovered and $\frac{y}{\dot{y}^{des}} \to \frac{1}{s}$. While this result may not be particularly interesting when dealing with rigid body dynamics, its real value is recognized when the flexible mode dynamics are explored.

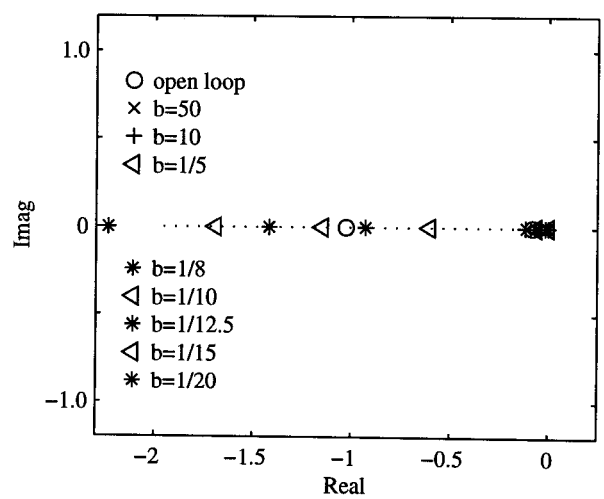

Figure 2. Short period closed loop poles as a changes.

$$W = \frac{1}{as+1}$$

$$\frac{y}{\dot{y}^{des}} = \frac{q_{ma}}{\dot{q}_{ma}^{des}} = \frac{s^2 + \left(\frac{1}{a} - Z_w + M_w \frac{Z_\delta}{M_\delta}\right)s + \frac{Z_\delta M_w - Z_w M_\delta}{aM_\delta}}{s\left[s^2 + \left(\frac{1}{a} - M_q - Z_w\right)s + \left(Z_w M_q - Z_q M_w + \frac{Z_\delta M_w - Z_w M_\delta}{aM_\delta}\right)\right]} \tag{7}$$

Consider a similar SISO system setup, but this time dealing with typical second-order flexible mode dynamics

$$\begin{bmatrix}\ddot{\eta}\\ \dot{\eta}\end{bmatrix}=\begin{bmatrix}-2\zeta\omega & -\omega^2\\ 1 & 0\end{bmatrix}\begin{bmatrix}\dot{\eta}\\ \eta\end{bmatrix}+\begin{bmatrix}E_\delta\\ 0\end{bmatrix}\delta$$

$$W=\frac{1}{bs+1}$$

$$\frac{y}{\dot{y}^{des}}=\frac{\dot{\eta}}{\ddot{\eta}^{des}}=\frac{1/b}{s^2+\left(\frac{1}{b}+2\zeta\omega\right)s+\omega^2} \tag{8}$$

$$\rightarrow \hat{\omega}=\omega,\ \text{and}\ \hat{\zeta}=\zeta+\frac{1}{2\omega b}$$

The resulting closed loop system dynamics are again altered by the introduction of a filter W. As equation 8 clearly shows, the damping of the closed loop elastic mode is controlled by the time constant of the filter W that modifies the standard dynamic inversion procedure. The change in the damping and hence the movement of the elastic mode dipole is illustrated in figure 3. For the values of $b>1$, the elastic mode dipole barely moves from the open loop dynamics. However for $b<1$, there is a pronounced movement in the poles along the line of constant frequency and increasing damping for diminishing b. In fact, for $b=1/17.5$, the damping becomes supercritical and the elastic mode dipole becomes a pair of real poles that approach s=0, 1/b in the limit and recovering the pole-zero cancellation with $\frac{y}{\dot{y}^{des}}\rightarrow\frac{1}{s}$. This observation that an addition of a filter into a dynamic inversion loop influences damping in a SISO system is carried through to a MIMO system where we combine short period and elastic mode dynamics.

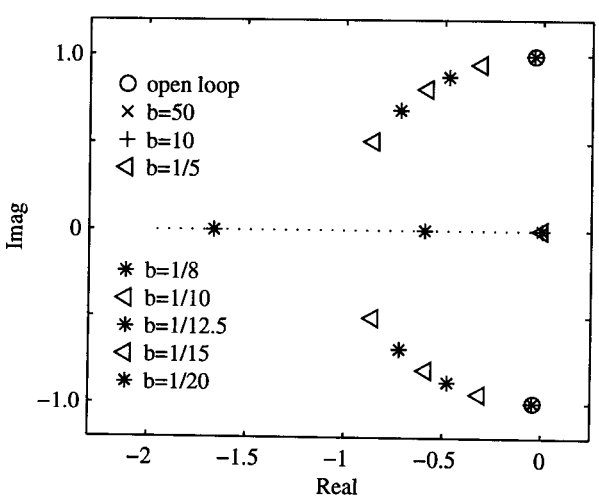

Figure 3. Flexible mode closed loop poles as b changes.

The SISO examples of equations 7 and 8 are equivalent to placing unmodeled first order actuator dynamics in the dynamic inversion control. One would expect that as the actuator bandwidth increases the $\frac{y}{\dot{y}^{des}}\rightarrow\frac{1}{s}$, which is precisely the case.

The combined MIMO system open loop dynamics are given by equations 1 and 2. The addition of the matrix W into the feedforward loop modifies the results of the standard dynamic inversion. Let W be a diagonal matrix of first order filters given by equation 9, which can also be expressed in state space system as shown.

$$W=\begin{bmatrix}\frac{1}{as+1} & 0\\ 0 & \frac{1}{bs+1}\end{bmatrix}$$

$$\begin{bmatrix}\dot{x}_a\\ \dot{x}_b\end{bmatrix}=\begin{bmatrix}-\frac{1}{a} & 0\\ 0 & -\frac{1}{b}\end{bmatrix}\begin{bmatrix}x_a\\ x_b\end{bmatrix}+\begin{bmatrix}\frac{1}{a} & 0\\ 0 & \frac{1}{b}\end{bmatrix}\bar{u} \tag{9}$$

$$\dot{\bar{x}}=\bar{A}\bar{x}+\bar{B}\bar{u}$$

$$\bar{y}=\bar{x}\ \text{and}\ \bar{u}=\dot{y}^{des}-CAx$$

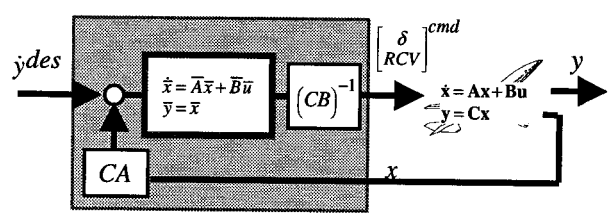

Figure 4. Modified dynamic inversion with dynamics in the modification matrix W

The block diagram that illustrates this modification is given in figure 4. Combining the modified dynamic inversion with the aircraft gives the following set of dynamics, expressed in matrix notation and shown in equation 10.

$$\begin{bmatrix}\dot{x}\\ \dot{\bar{x}}\end{bmatrix}=\begin{bmatrix}A & B(CB)^{-1}\\ -\bar{B}CA & \bar{A}\end{bmatrix}\begin{bmatrix}x\\ \bar{x}\end{bmatrix}+\begin{bmatrix}0\\ \bar{B}\end{bmatrix}\dot{y}^{des}$$

$$y=\begin{bmatrix}C & 0\end{bmatrix}\begin{bmatrix}x\\ \bar{x}\end{bmatrix} \tag{10}$$

Clearly equation 10 shows that as expected the dynamics of filter W alter the closed loop dynamics. After some algebraic manipulation we get a very large and messy analytical expression for the closed loop poles. In order to understand how first order filter matrix influences the dynamic inversion inner loop, it is instructive to look at the pole movement while holding one of the time constants fixed and changing the other. Looking at the numeric values of the closed loop poles,

it becomes immediately apparent that for $a \neq 0$ and $b \neq 0$ two of the six poles are integrators. Another pole maintains a value in the neighborhood of $1/a$. However, there are no longer poles coincident with open loop transmission zeros, so there is no pole-zero cancellation.

Figures 5 and 6 illustrate the pole movement as the filter time constants are varied. In Figure 5, b is fixed and a is allowed to vary over the same range as was previously shown in figure 2. Notice that short period poles move in the manner similar to that observed in the SISO short period case, while the flexible mode dipole remains essentially fixed in the neighborhood that is specified by the given value of b. In fact the movement of the faster of the two short period poles is clearly visible in the figure. Similar phenomenon is observed in figure 6, where a is fixed and b is allowed to vary. The short period dynamics remain essentially fixed near the origin while the elastic mode dipole travels along fixed frequency and increasing damping with decreasing value of b. Again this is similar to what has been observed in the SISO elastic mode case and shown in figure 3.

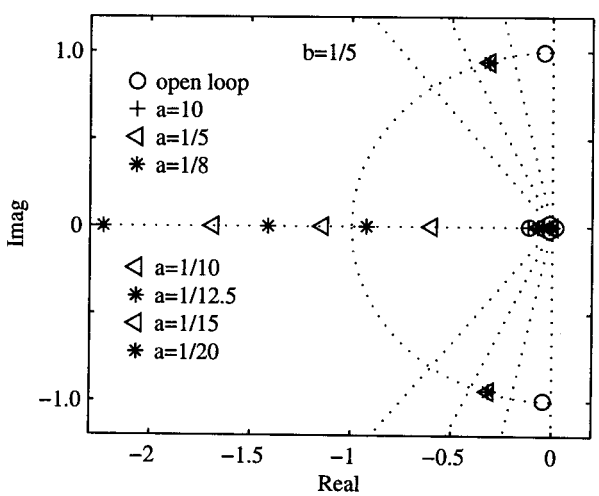

Figure 5. Closed loop poles for short period + 1 flexible mode w/ a changing, b=1/5.

The fact that while one filter time constant is fixed while the other can be varied to manipulate a set of dynamics that are of interest is very useful in design. At first glance, it would not be surprising that the time constants modify the system in the decoupled manner described. There is some frequency separation between the short period and the elastic dynamics. Furthermore, q_{ma} is predominantly rigid body whereas q_{ps}-q_{ma} is predominantly elastic based. However, the frequency separation causing decoupling is a very deceptive conclusion in this case as examination of full longitudinal plus flexible mode dynamics will show.

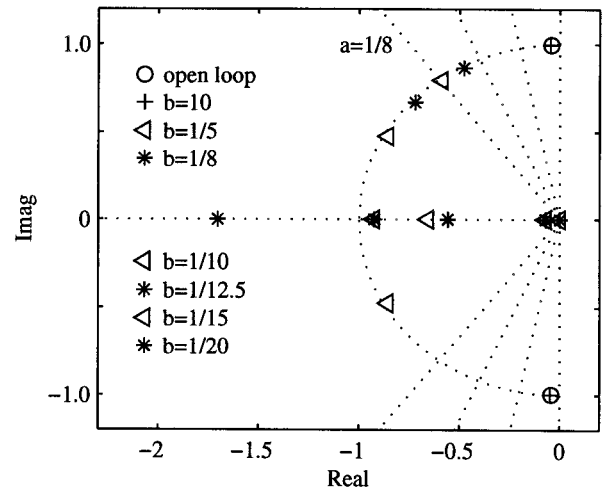

Figure 6. Closed loop poles for short period + 1 flexible mode w/ b changing, a=1/8.

Adding Complexity

Consider the full longitudinal model with a single flexible mode. Retaining the same control variables as used above in equation 2, the system dynamics are given by equation 11

$$\begin{bmatrix} \dot{u} \\ \dot{w} \\ \dot{q} \\ \dot{\theta} \\ \ddot{\eta} \\ \dot{\eta} \end{bmatrix} = \begin{bmatrix} X_u & X_w & X_q & X_\theta & 0 & 0 \\ Z_u & Z_w & Z_q & Z_\theta & Z_\eta & Z_{\dot{\eta}} \\ M_u & M_w & M_q & M_\theta & M_\eta & M_{\dot{\eta}} \\ 0 & 0 & 1 & 0 & 0 & 0 \\ 0 & E_w & E_q & 0 & -2\varsigma\omega & -\omega^2 \\ 0 & 0 & 0 & 0 & 1 & 0 \end{bmatrix} \begin{bmatrix} u \\ w \\ q \\ \theta \\ \dot{\eta} \\ \eta \end{bmatrix} + \begin{bmatrix} X_\delta & 0 \\ Z_\delta & Z_{rcv} \\ M_\delta & M_{rcv} \\ 0 & 0 \\ E_\delta & E_{rcv} \\ 0 & 0 \end{bmatrix} \begin{bmatrix} \delta \\ RCV \end{bmatrix} \tag{11}$$

Following the same process as before, the direct dynamic inversion produces results seen in equation 4. The closed loop poles are given in expression 12

$$\begin{Bmatrix} \pm\ u-w \text{ dynamics} \\ 0,\ 0,\ 0,\ 0 \end{Bmatrix} \tag{12}$$

The closed loop poles are a set comprised of 4 poles of internal dynamics that coincide with open loop transmission zeros of the system in equation 11 and of two poles at s=0 which correspond to the integrators found in equation 4. The closed loop system dynamics from $\dot{y}^{des}$ to $\dot{y}$ are given by equation 13. From this equation it is apparent that the controlled variables are independent of the u-w dynamics. Furthermore, the steady-state system internal dynamics are described by

motion on the u-w-η-manifold.

$$\begin{bmatrix} \dot{u} \\ \dot{w} \\ \dot{q} \\ \dot{\theta} \\ \ddot{\eta} \\ \dot{\eta} \end{bmatrix} = \begin{bmatrix} \overline{X}_u & \overline{X}_w & \overline{X}_q & \overline{X}_\theta & X_{\dot{\eta}} & Z_\eta \\ \overline{Z}_u & \overline{Z}_w & \overline{Z}_q & \overline{Z}_\theta & \overline{Z}_{\dot{\eta}} & \overline{Z}_\eta \\ 0 & 0 & 0 & 0 & 0 & 0 \\ 0 & 0 & 1 & 0 & 0 & 0 \\ 0 & 0 & 0 & 0 & 0 & 0 \\ 0 & 0 & 0 & 0 & 1 & 0 \end{bmatrix} \begin{bmatrix} u \\ w \\ q \\ \theta \\ \dot{\eta} \\ \eta \end{bmatrix} + \begin{bmatrix} \overline{X}_{\dot{y}1} & \overline{X}_{\dot{y}2} \\ \overline{Z}_{\dot{y}1} & \overline{Z}_{\dot{y}2} \\ 1 & \overline{M}_{\dot{y}2} \\ 0 & 0 \\ 0 & \overline{E}_{\dot{y}2} \\ 0 & 0 \end{bmatrix} \begin{bmatrix} \dot{y}_1 \\ \dot{y}_2 \end{bmatrix}^{des} \tag{13}$$

$$\begin{bmatrix} \dot{y}_1 \\ \dot{y}_2 \end{bmatrix} = \begin{bmatrix} \dot{y}_1^{des} + \left(\overline{M}_{\dot{y}2} + \phi'\overline{E}_{\dot{y}2}\right)\dot{y}_2^{des} \\ \Delta\phi'\overline{E}_{\dot{y}2}\dot{y}_2^{des} \end{bmatrix} = \begin{bmatrix} \dot{y}_1^{des} \\ \dot{y}_2^{des} \end{bmatrix}$$

where $\overline{M}_{\dot{y}2} = -\phi'\overline{E}_{\dot{y}2}$ and $\Delta\phi'\overline{E}_{\dot{y}2} = 1$

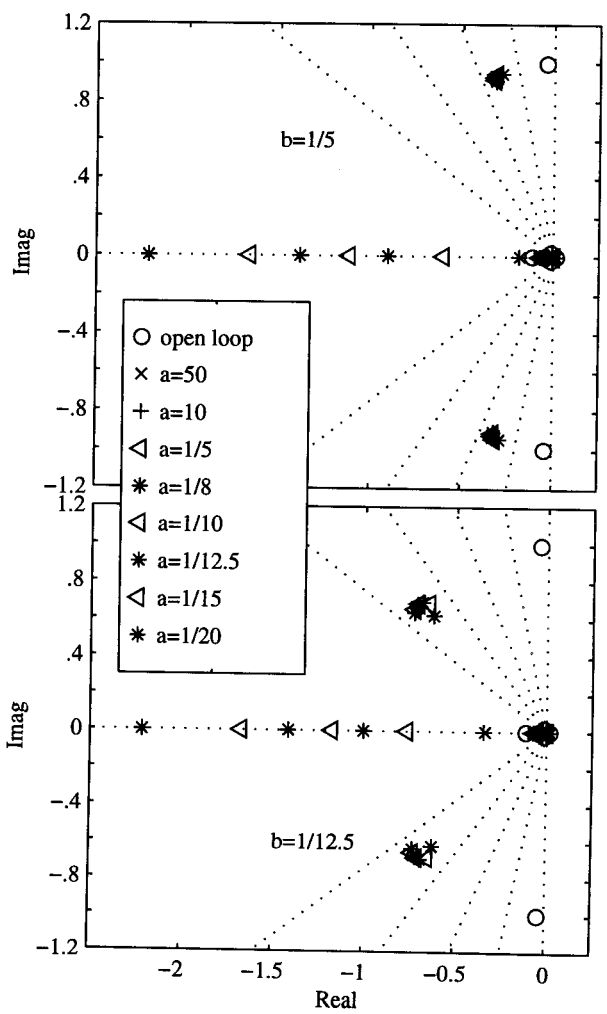

Figure 7. Longitudinal + 1 mode w/ *a* changing.

If we introduce modification to the dynamic inversion as shown in the earlier section, the result is no longer a clean separation as has been observed with short period approximation and an elastic mode. The closed loop A matrix structure resembles the more fully populated one of the open loop (eqn. 11) rather than the nice decoupled one of the closed loop (eqn. 13). The pole movement associated with changing time constants of the transfer matrix W is shown in figures 7 and 8. The closed loop poles structure of $\{*, *, *, *, *, *, 0, 0\}$ applies to both of the figures.

For changing *a*, time constant of the measured mean axis pitch rate, there is the expected movement of the longitudinal poles that has been previously seen in figures 2 and 5, but there is also some minor movement of the flexible mode as illustrated in figure 7. When the value of *b* is allowed to change, as shown in figure 8, the flexible mode follows the now familiar pattern witnessed in figures 3 and 6 of changing damping along a constant frequency. However, there is also movement of longitudinal poles, the extent of which depends on

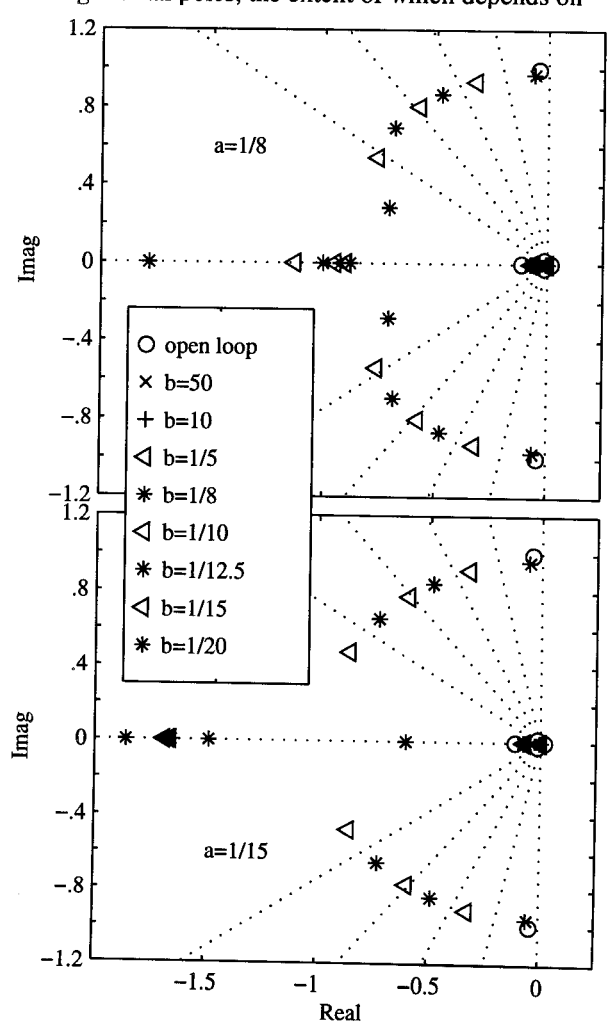

Figure 8. Longitudinal + 1 mode w/ *b* changing.

the value of a. This begins to constrain some of the decoupling freedom in our control design. Taking another step towards a real flexible aircraft, an additional level of complexity is introduced in the following section.

Additional flexible modes

Consider the longitudinal equations of motion shown in equation 11, which are augmented by 3 additional flexible modes with all the associated interdependencies of rigid and elastic dynamics as well as inter mode dependencies. Thus, the system dynamics consist of 12 states and retain the same control variables as have been used throughout. In the now familiar process, we keep one of the time constants in W fixed while varying the other. The results are illustrated in figures 9 and 10. For a changing a with constant b, figure 9 shows the movement of short period poles while all but one flexible mode remain clustered near their open loop positions. The pole corresponding to the primary fuselage bending mode

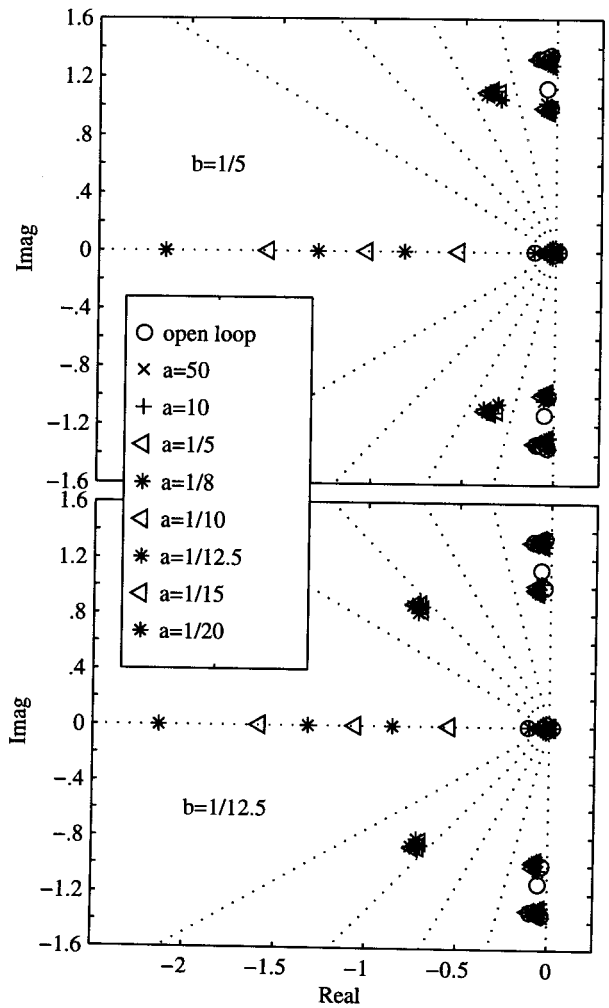

Figure 9. Longitudinal + 4 modes w/ a changing.

has migrated away from its open loop position to a higher damping. When b is changing while a is held constant, the pole movement, illustrated in figure 10, is similar to the one observed in the prior section. The poles of the flexible modes that are not primarily fuselage modes, modes 1, 3, and 4, form tight clusters around their open loop positions. The primary fuselage bending mode poles, mode 2, follow the previously established movement pattern of increased damping with decreasing b along what is essentially a constant frequency. There is also movement from the rigid body poles with the amount dependent on the value of constant a.

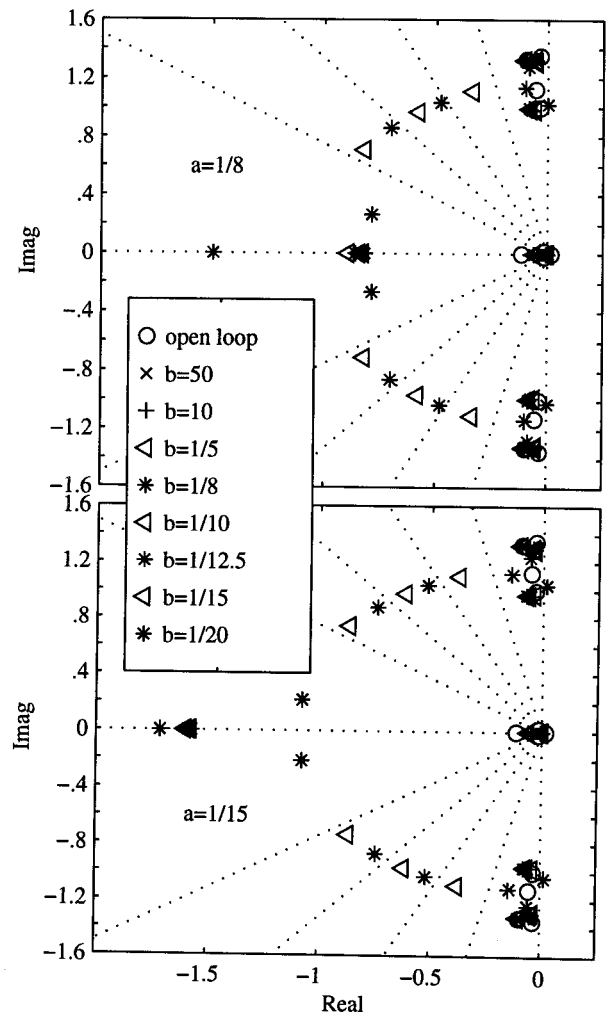

Figure 10. Longitudinal + 4 modes w/ b changing.

Hence, the introduction of additional modes to the dynamics has not changed the observed general pattern of behavior from either rigid body or flexible dynamics. The additional flexible modes do not significantly alter the dependence of the primary flexible mode on the W time constant b, nor do they have a large influence on the interaction between rigid body and flexible mode dynamics. From the physics perspective of this

problem, this result is not surprising, since the additional flexible modes are primarily wing modes and are not significantly affected by the fuselage mounted control surfaces considered here. Similar behavior has been observed with a much higher number of elastic modes, some of which were fuselage modes, but beyond effective power of the controller. Thus it appears that a reasonable independence of control still exists for longitudinal plus flexible mode system dynamics under the dynamic inversion modification described in this paper. Granted this apparent separation exists in a perfect world, and once unmodeled dynamics as well as actuator dynamics are introduced the separation is not as clean, however, enough decoupling still exists to allow for a great deal of controller tuning to be done through W. [6]

The analytical expression for the transfer function matrix, not shown here, is no longer a diagonal set of integrators but instead is a fully populated matrix. This follows, as it did in SISO system, from the fact that introducing additional dynamics into the dynamic inversion loop precludes the pole-zero cancellation required to give the diagonal set of integrators. While not as elegant mathematically, this result allows control of flexible mode damping and thus tailor the disturbance response of the closed loop in addition to the commanded variable response.

Adding uncertainty in flexible mode

As with any control methodology, the issue of robustness must be addressed. The work in reference 6 considered parametric uncertainty in the frequency and damping of the primary fuselage flexible mode. It was found that the modified dynamic inversion methodology produced a controller with good stability robustness to the indicated uncertainty. In this section, we revisit the dynamics discussed earlier in this paper and consider the effects parametric uncertainty in frequency and damping of a flexible mode has on the closed inner loop behavior of the system.

Consider for clarity, the simplest available set of dynamics, those of short period plus 1 flexible mode described by equations 1 and 2, and introduce damping and frequency multiplicative uncertainty given below

$$\omega \to \omega(1+\Delta_\omega) \quad \text{where } \Delta_\omega \in \{\delta : |\delta| \le 1, \delta \in \Re\}$$
$$\varsigma \to \varsigma(1+\Delta_\varsigma) \quad \text{where } \Delta_\varsigma \in \{\delta : |\delta| \le 1, \delta \in \Re\}$$

The closed loop dynamics associated with the standard dynamic inversion are given in equation 15. Note that the difference between nominal (eqn. 5) and perturbed closed loop system is in the $\ddot{\eta}$ equation with appearance of $2\overline{\varsigma\omega}$ and $\overline{\omega}^2$ terms. Both are dependent on the nominal frequency and damping as well as the introduced uncertainty (eqn. 15).

$$\begin{bmatrix} \dot{w} \\ \dot{q} \\ \ddot{\eta} \\ \dot{\eta} \end{bmatrix} = \begin{bmatrix} \overline{Z}_w & \overline{Z}_q & \overline{Z}_{\dot{\eta}} & \overline{Z}_\eta \\ 0 & 0 & 0 & 0 \\ 0 & 0 & 2\overline{\varsigma\omega} & \overline{\omega}^2 \\ 0 & 0 & 1 & 0 \end{bmatrix} \begin{bmatrix} w \\ q \\ \dot{\eta} \\ \eta \end{bmatrix} + \begin{bmatrix} \overline{Z}_{\dot{y}1} & \overline{Z}_{\dot{y}2} \\ 1 & \overline{M}_{\dot{y}2} \\ 0 & \overline{E}_{\dot{y}2} \\ 0 & 0 \end{bmatrix} \begin{bmatrix} \dot{y}_1 \\ \dot{y}_2 \end{bmatrix}^{des} \tag{15}$$

where $\overline{\omega} = (2\omega\Delta_\omega)^{1/2}$ and $\overline{\varsigma} = \dfrac{\omega\Delta_\varsigma + \varsigma\Delta_\omega}{(2\omega\Delta_\omega)^{1/2}}$

The transfer function of the closed inner loop dynamics, shown in equation 16, is no longer the integrator chain seen in equation 4.

$$\begin{bmatrix} y_1 \\ y_2 \end{bmatrix} = \begin{bmatrix} \dfrac{1}{s} & \dfrac{-\phi'(2\overline{\varsigma\omega}s + \overline{\omega}^2)}{(s^2 + 2\overline{\varsigma\omega}s + \overline{\omega}^2)} \\ 0 & \dfrac{s}{s^2 + 2\overline{\varsigma\omega}s + \overline{\omega}^2} \end{bmatrix} \begin{bmatrix} \dot{y}_1^{des} \\ \dot{y}_2^{des} \end{bmatrix} \tag{16}$$

And the closed loop poles associated with the perturbed system are described in expression 17.

$$\left\{ \overline{Z}_w,\ 0,\ -\overline{\varsigma\omega} \pm \left(\overline{\omega}^2(\overline{\varsigma}^2 - 1)\right)^{1/2} \right\} = \left\{ \begin{array}{l} Z_w + Z_\delta \left(\dfrac{E_w M_{rcv} - E_{rcv} M_w}{E_\delta M_{rcv} - E_{rcv} M_\delta} \right) \\ \qquad + Z_{rcv} \left(\dfrac{E_\delta M_w - E_w M_\delta}{E_\delta M_{rcv} - E_{rcv} M_\delta} \right), \quad 0 \\ -\omega\Delta_\varsigma - \varsigma\Delta_\omega \\ \pm\left(\omega^2\Delta_\varsigma^2 + 2\omega\varsigma\Delta_\varsigma\Delta_\omega + \varsigma^2\Delta_\omega^2 - 2\omega\Delta_\omega\right)^{1/2} \end{array} \right\} \tag{17}$$

Since the nature of the uncertainty did not change the open loop transmission zeros and this is a direct dynamic inversion, the first two poles coincide with the open loop transmission zeros as was seen earlier in expression 6. The two integrators, however, have changed into poles that are a function of $\overline{\varsigma}$ and $\overline{\omega}$, which are given in terms of their components in expression 17. As is evident from equation 15, the w internal dynamics remain independent of attitude dynamics and are only indirectly influenced by the flexible mode uncertainty through state variables $\dot{\eta}$ and η in the $\dot{w}$ equation. This is also confirmed by coincidence of transmission zeros with closed loop poles.

The same observation holds for a full longitudinal system with a flexible mode. The closed loop dynamics of direct dynamic inversion are given in equation 18.

Again the difference between the nominal closed loop (eqn. 13) and the perturbed system resides in the $\ddot{\eta}$ equation with reappearance of $2\overline{\varsigma\omega}$ and $\overline{\omega}^2$ terms.

$$\begin{bmatrix} \dot{u} \\ \dot{w} \\ \dot{q} \\ \dot{\theta} \\ \ddot{\eta} \\ \dot{\eta} \end{bmatrix} = \begin{bmatrix} \overline{X}_u & \overline{X}_w & \overline{X}_q & \overline{X}_\theta & X_{\dot{\eta}} & Z_\eta \\ \overline{Z}_u & \overline{Z}_w & \overline{Z}_q & \overline{Z}_\theta & \overline{Z}_{\dot{\eta}} & \overline{Z}_\eta \\ 0 & 0 & 0 & 0 & 0 & 0 \\ 0 & 0 & 1 & 0 & 0 & 0 \\ 0 & 0 & 0 & 0 & 2\overline{\varsigma\omega} & \overline{\omega}^2 \\ 0 & 0 & 0 & 0 & 1 & 0 \end{bmatrix} \begin{bmatrix} u \\ w \\ q \\ \theta \\ \dot{\eta} \\ \eta \end{bmatrix} + \begin{bmatrix} \overline{X}_{\dot{y}1} & \overline{X}_{\dot{y}2} \\ \overline{Z}_{\dot{y}1} & \overline{Z}_{\dot{y}2} \\ 1 & \overline{M}_{\dot{y}2} \\ 0 & 0 \\ 0 & \overline{E}_{\dot{y}2} \\ 0 & 0 \end{bmatrix} \begin{bmatrix} \dot{y}_1 \\ \dot{y}_2 \end{bmatrix}^{des} \tag{18}$$

$$\begin{bmatrix} \dot{y}_1 \\ \dot{y}_2 \end{bmatrix} = \begin{bmatrix} \dot{y}_1^{des} + \phi'\left(2\overline{\varsigma\omega}\dot{\eta} + \overline{\omega}^2\eta\right) \\ \dot{y}_2^{des} + \Delta\phi'\left(2\overline{\varsigma\omega}\dot{\eta} + \overline{\omega}^2\eta\right) \end{bmatrix}$$

The transfer function of the closed inner loop dynamics, shown in equation 19, is very similar to the one for short period found in equation 16. There is no longer a chain of integrators present. However, in the limit as $\Delta_\varsigma \to 0$ and $\Delta_\omega \to 0$ the chain of integrators, as seen in equation 4 is recovered.

$$\begin{bmatrix} y_1 \\ y_2 \end{bmatrix} = \begin{bmatrix} \dfrac{1}{s} & \dfrac{-\phi'\left(2\overline{\varsigma\omega}s + \overline{\omega}^2\right)}{\Delta\phi' s\left(s^2 + 2\overline{\varsigma\omega}s + \overline{\omega}^2\right)} \\ 0 & \dfrac{s}{s^2 + 2\overline{\varsigma\omega}s + \overline{\omega}^2} \end{bmatrix} \begin{bmatrix} \dot{y}_1^{des} \\ \dot{y}_2^{des} \end{bmatrix} \tag{19}$$

The first four closed loop poles, described in equation 20 correspond to open loop transmission zeros which is similar to the observed behavior of the short period system and show no dependence of internal dynamics on the uncertainty. The two remaining poles changed from dynamic inversion produced integrators to functions of uncertainty, again in a manner similar to the short period system.

$$\left\{ \begin{array}{l} \pm\ u - w \text{ dynamics, } 0,\ 0, \\ -\omega\Delta_\varsigma - \zeta\Delta_\omega \\ \pm\left(\omega^2\Delta_\varsigma^2 + 2\omega\zeta\Delta_\varsigma\Delta_\omega + \zeta^2\Delta_\omega^2 - 2\omega\Delta_\omega\right)^{1/2} \end{array} \right\} \tag{20}$$

Thus when uncertainty is added into the direct dynamic inversion, whether the system is short period approximation or the full longitudinal model, the resulting closed loop dynamics are governed by the open loop transmission zeros and flexible mode uncertainty. This points to a potentially serious issue with stability of direct dynamic inversion. System stability is affected by uncertainty in the dynamics far separated in frequency from the dynamics that actually go unstable. In this case, flexible mode uncertainty could drive one of the dynamic inversion integrator poles unstable for large enough Δ_ς and Δ_ω. The existence of potentially unstable closed loop poles confirms the disadvantage of direct inversion especially with lightly damped dynamics of the flexible modes.

For control design there are two question that are important to consider. The first is what happens for a given controller designed using the modified dynamic inversion as a range of uncertainty is considered. The second is does enough decoupling between the rigid body and flexible mode dynamics still exist so that time constants of the matrix W might be used to tune the controller.

To answer the first question consider longitudinal dynamics with one flexible uncertain mode in the context of modified dynamic inversion. The plot in figure 11 illustrates the pole migration for changing frequency uncertainty while maintaining a constant damping uncertainty and a fixed value of *a* and *b* time constants of W. The frequency uncertainty is used because it has been found in previous work to be the driving factor. Also, the decreasing frequency of the flexible mode is causing instability that happens at low frequency. However, recall that the nature of $\dot{y}^{des}$ dynamics has a pronounced affect on the overall system stability that is not taken into consideration in this analysis. In reference 6, the low frequency dynamics were not as sensitive to uncertainty due to the use of second order filters in the W modification matrix. The

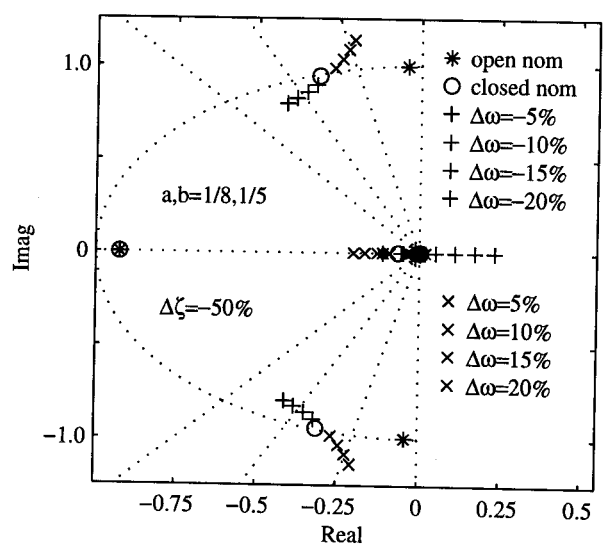

Figure 11. Closed loop poles for longitudinal + 1 flexible mode w/ {a,b,Δζ} constant, Δω,vaying. .

influence of second order filters is not discussed in this paper.

To address the second question, consider again the longitudinal plus one flexible mode dynamics (eqn. 11) and apply modified dynamic inversion. In order to explicitly consider system uncertainty during the design phase, a controller is designed on a nominal system and then applied to a system perturbed in flexible mode frequency and damping. Once the uncertainty parameter boundaries are set, the affect of independent manipulation of the *a* and *b* time constants of the matrix W on the behavior of the closed loop system is explored. This behavior is illustrated in figures 12 and 13. It is interesting to note that in figure 12 while *a* is varied with *b* fixed the rigid body poles move while the flexible mode remains completely stationary unlike the clustering observed in figure 7 where no uncertainty was present in the system. The low frequency rigid body pole also seems to be immune to the variation in *a*. This would imply that the closed

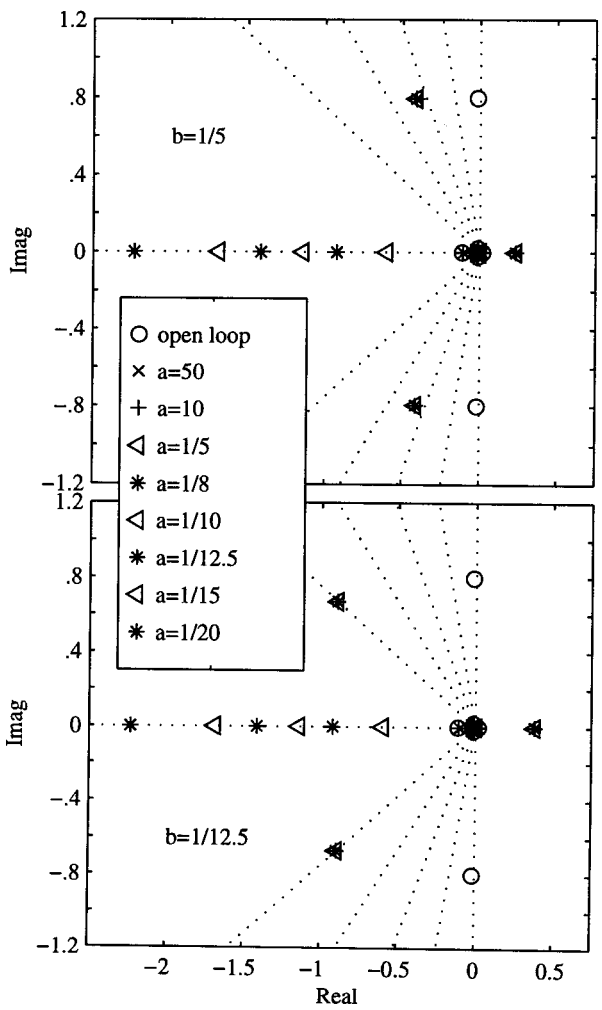

Figure 12. Longitudinal + 1 mode w/ $\{\Delta\zeta,\Delta\omega\}=\{-20\%, -50\%\}$ *a* changing, *b*=1/5, 1/12.5.

loop flexible mode associated poles are dominated by uncertainty and *b*, unlike the nominal case where *a* had a minor influence.

In figure 13, the time constant *b* is varied while *a* remains fixed. The results show the higher frequency rigid body dynamics remain fixed contrary to what was observed in figure 8 when no uncertainty was present. The flexible mode no longer follows the familiar pattern of changing damping along constant frequency. It now changes both frequency and damping with changing *b*. The low frequency rigid body pole also moves with changing *b*, becoming more unstable with smaller *b*.

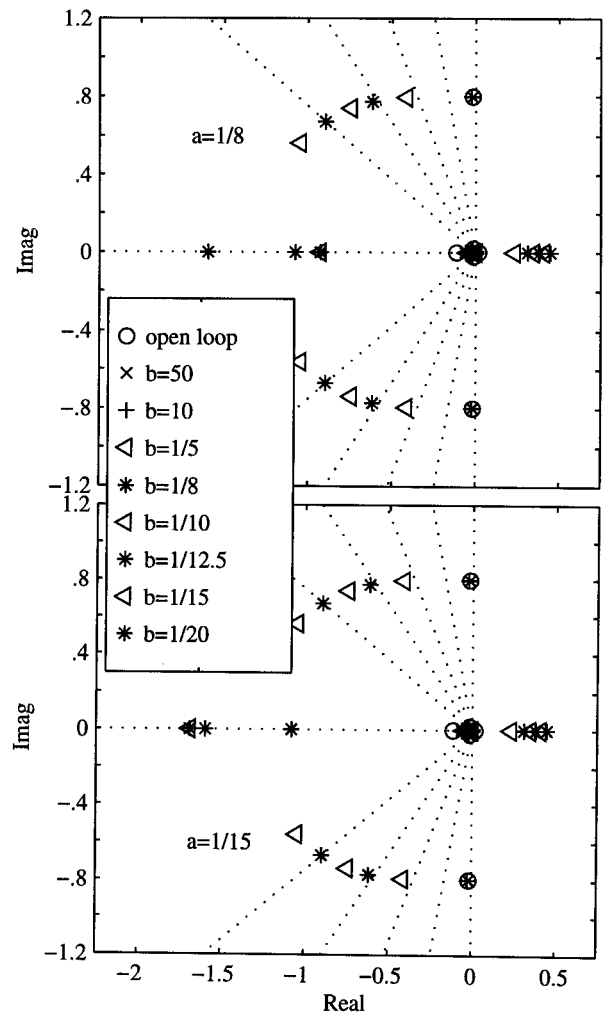

Figure 13. Longitudinal + 1 mode w/ $\{\Delta\zeta,\Delta\omega\}=\{-20\%, -50\%\}$ *b* changing, *a*=1/8,1/15

This observed behavior suggests that the presence of uncertainty overwhelms the influence of the modification matrix W on the low frequency rigid body dynamics. The effect on the controller design is somewhat limiting in that very low frequency dynamics must now be carefully considered when attempting to specify the desired flexible mode damping via the

adjustment of the b time constant of the matrix W. As previously mentioned, the problem is somewhat mitigated by the use of second order filters on the diagonal of W [6] as well as the effect of the $\dot{y}^{des}$ dynamics on overall closed loop stability.

Conclusion

The modification introduced into the standard dynamic inversion methodology first discussed in reference 6 has been analytically explored on longitudinal and symmetric flexible dynamics of varying complexity. While the model used here is much simpler than the full model for which the controller introduced in reference 6 was designed, the results are revealing nonetheless. This paper begins to provide some analytical basis and further insight into the workings of dynamic inversion methodology that has been modified to address the problem associated with these large, flexible transports.

There exists to a large degree freedom to control rigid body and flexible dynamics independently of one another in the modified dynamic inversion context. The apparent separation in controlling the short period and elastic mode dynamics through modified dynamic inversion is valuable when control of disturbances is as important as control of commanded variable. Specifically, the ability to alter the damping of elastic modes as well as cancel their response to the commanded vehicle motion is the main objective of an integrated flight/structural mode control that is required for advanced, large, flexible aircraft.

The increased complexity of system dynamics that included full longitudinal as well as multiple symmetric flexible mode dynamics show that certain degree of separation in controlling rigid body and flexible dynamics still exist. However, the introduction of parametric uncertainty into frequency and damping of the dominant flexible mode, also showed the coupling between very low frequency rigid body and flexible dynamics. This coupling must be carefully considered during a controller design process since in the real world application there are always uncertainty present in the system. In fact, the results presented in this paper have been used to design a series of controllers undergoing testing in real time piloted simulation.

References

[1] Wykes, John, Byar, Thomas, MacMiller, Cary, and David Greek. Analyses and Tests of the B-1 Aircraft Structural mode Control System. NASA CR 144887. 1980.

[2] Newman, Brett, and Carey Buttrill. "Conventional Control for an Aeroelastic, Relaxed Static Stability high-Speed Transport." AIAA paper 95-3250-CP.

[3] Bugajski, Daniel, Dale Enns, and Russ Hendrick. Multi-Application Control (MACH): F-18 High Angle-of-Attack Research Vehicle (HARV) Reports. Honeywell Technology Center. November, 1994.

[4] Application of Multivariable Control Theory to Aircraft Control Laws. Final Report: Multivariable Control Design Guidelines. WL-TR-96-3099. May 1996.

[5] Enns, Dale, Dan Bujaski, Russ Hendrick, and Gunter Stein. "Dynamic Inversion: An Evolving Methodology for Flight Control Design." Int. J. Control, 1994, Vol. 59, No. 1, 71-91.

[6] Gregory, Irene M. "Dynamic Inversion to Control Large Flexible Transport Aircraft." 1998 AIAA Guidance, Navigation, and Controls Conference, Boston, MA. AIAA paper 98-4323.

[7] Etkin, B. Dynamics of Aerodynamic Flight. Wiley. 1956.